

A generalized framework for quantum subspace diagonalization

Paul D. Nation,^{1,*} Abdullah Ash Saki,² and Hwajung Kang¹

¹IBM Quantum, IBM T. J. Watson Research Center, Yorktown Heights, NY 10598 USA

²IBM Quantum, IBM Research Cambridge, Cambridge, MA 02142 USA

(Dated: March 20, 2026)

We present a framework for computing the solution to Hamiltonian eigenproblems in a subspace defined by bit-strings sampled from a quantum computer. Hamiltonians are represented using an extended alphabet that includes projection and ladder operators, yielding a unified solution method for qubit and fermionic systems. Operators are grouped and sorted so that only non-zero terms are evaluated and a minimal number of subspace lookup operations are performed. Bit-strings are expressed using bit-sets to reduce memory consumption and allow for evaluating operators with no intrinsic limitation on the number of qubits. Subspaces defined over bit-sets are stored in a hash map format that allows for efficient indexing and lookup operations. Our method can be used to directly construct sparse matrix representations or obtain matrix-free solutions. Users are free to utilize these in their eigensolver of choice. We show the benefits of our framework by computing the ground-state solution to examples from condensed matter physics and quantum chemistry with less memory and runtime compared to existing techniques, in some cases by an order of magnitude or more. This work provides a flexible interface for performant quantum-classical eigensolutions for candidate quantum advantage applications.

Eigenvalue problems represent one of the mainstay calculations for near-term [1, 2] and fault-tolerant [3–7] quantum applications, including domains such as quantum chemistry [8, 9] and quantum optimization [10]. Recent demonstrations have shown that such techniques offer promise towards achieving quantum advantage using pre-fault tolerant quantum hardware [11–21], where eigensolutions are formulated within a subspace defined by bit-strings sampled from a quantum computer and leverage classical computing resources to perform the eigenvalue computation itself.

These methods aim to solve eigenproblems of the form $\hat{H}|\psi_j\rangle = \lambda_j|\psi_j\rangle$, or the generalized version $\hat{H}|\psi_j\rangle = \lambda_j M|\psi_j\rangle$, where \hat{H} is the Hamiltonian of a qubit or fermionic system, λ_j and $|\psi_j\rangle$ are the target eigenvalue and eigenvector, respectively, and M is a possible modal matrix [22]. The state $|\psi_j\rangle$ is defined in a subspace spanned by the counts returned from sampling one or more quantum circuits on a quantum processor. Implicit in these methods is that $|\psi_j\rangle$ have compact support over the Hilbert space, allowing for accurate sampling with only a polynomial number of circuit repetitions, and any possible quantum advantage requires sampling bit-strings pertinent to the target eigenstate faster on a quantum computer than counterpart classical algorithms. With a Hamiltonian represented in the computational basis, such problems can readily be cast as sparse matrix eigenproblems that are amenable to a variety of classical solution methods such as ARPACK [23], PRIMME [24], and SLEPC [25]. At their core, these sparse eigensolution methods require repeatedly solving sparse matrix-vector products (SpMV), and the conversion of Hamiltonian operators and subspaces of bit-strings into data structures

compatible with efficient SpMV operations is a key step in these workflows [26]. Because only the output vector from SpMV is utilized, matrix-free methods that require no explicit matrix storage can also be used provided computing individual matrix-elements is efficient.

Current quantum subspace diagonalization (QSD) approaches are, in general, tied to a domain-specific application area and are not generally applicable to other problem instances. For example, quantum chemistry has a well-versed set of tools for solving the eigenstates of fermionic systems [27–29], but that are incapable of addressing qubit Hamiltonians. Conversely, tools for solving qubit based systems also exist [30] and can solve fermionic systems as well, provided one performs a fermionic to qubit Hamiltonian transformation, e.g. a Jordan-Wigner transformation [31], but otherwise use independent solution methods and input / output formats. In addition, these QSD solvers are limited to ≤ 128 qubits due to restrictions on the number of bits that can be used to specify common integer data types. With quantum computing hardware already fielding qubit counts above this threshold, removing this limitation is important for solving problems at the frontier of quantum advantage and beyond.

In this work we present a generalized framework, called FULQRUM [32], for performing *both* qubit and fermionic QSD. This is accomplished by efficiently casting fermionic problems to qubit Hamiltonians consisting of an operator alphabet that includes an extended set of projection and ladder operators. Utilizing bit-sets for computational basis states, as opposed to integers, our method has no fundamental limit on the number of allowed qubits. FULQRUM does not perform eigensolving itself, instead generating canonical matrix representations that are compatible with a wide range of existing numerical methods, giving users a choice of classical eigensolver and related tools such as preconditioners and

* E-mail: paul.nation@ibm.com

matrix-reordering techniques leveraging both CPUs and GPUs. Although generalized solution techniques often come at the expense of performance, in terms of runtime, memory consumption, or both, here we will demonstrate that it is possible to outperform current implementations in terms of both metrics whilst maintaining flexibility.

I. RESULTS

In this work we utilize two computing platforms: "Computer A" is a 12-core, 24-thread AMD 7900 processor with 128 GiB of memory running Ubuntu 24.04, while "Computer B" is a 4-socket Intel Xeon Platinum 8260 (24-cores, 48 threads) workstation with 3 TiB of memory running Ubuntu 22.04. Here we highlight the flexibility of our framework and validate its performance by presenting results for solving the ground state eigensolution for both qubit and fermionic Hamiltonians.

To begin, we consider the following antiferromagnetic XXZ spin-1/2 chain Heisenberg model,

$$H = \sum_{i=1}^{L-1} J(X_i X_{i+1} + Y_i Y_{i+1}) + Z_i Z_{i+1},$$

where L is the number of sites and J is the coupling strength for the off-diagonal term, $X_i X_{i+1} + Y_i Y_{i+1}$, and set $J = 0.3$. To estimate the ground state energy for this Hamiltonian, we utilize Sample-based Krylov Quantum Diagonalization (SKQD) [16]. SKQD is a QSD algorithm for near-term quantum computers where the subspace is comprised of quantum Krylov states built from a set of time-evolved states generated from a reference state using the target Hamiltonian. Upon sampling the Krylov states, diagonalization of the Hamiltonian in the generated subspace is performed classically. We construct fifteen quantum circuits corresponding to different time steps incremented by $\Delta t = 0.1$ (trotter steps), starting from zero, for each $L \in \{30, 36, 40, 46, 50, 56, 60\}$, and evolve them from a reference Neel state, $|0101..01\rangle$. The minimum chain length is set such that meaningful timing information can be gathered, while the upper limit comes from the 64-qubit limit of the `qiskit-addon-sqd` [30] qubit Hamiltonian SQD eigensolver that we compare against. Although our comparison does not focus on accuracy, both models return numerically identical eigenvalues, to account for errors we post-process sampled bit-strings that are a Hamming distance one away from the Neel state; exploiting the conservation of total magnetization, total spin in the z -direction, in this model. Using these corrected bit-strings, we compare the performance of FULQRUM and `qiskit-addon-sqd` for projection of the Hamiltonian into the subspace, as well as classical eigensolving. Here we use FULQRUM's "fast" CSR matrix building mode, see Sec. (III C). For the diagonalization procedure, the SCIPY [33] eigensolver ARPACK [23] is used for both methods as this choice is hard-coded for the `qiskit-addon-sqd` qubit solver. In contrast, FULQRUM

allows the user to select their eigensolver of choice, potentially enabling more performant eigensolving as the method can be targeted to the Hamiltonian under consideration. Here a uniform vector is used as the initial vector passed to the eigensolver for both frameworks.

The SKQD benchmark is executed on Computer A and evaluated in terms of runtime and peak-memory usage. As the core differentiating routine is projection of the Hamiltonian into the target subspace, we focus on comparing the time taken in this step. However, the peak memory usage is measured over the full eigensolving workflow so as to faithfully capture the resources required to solve the complete problem. Results are displayed in Fig. (1) where we see that even at the smallest number

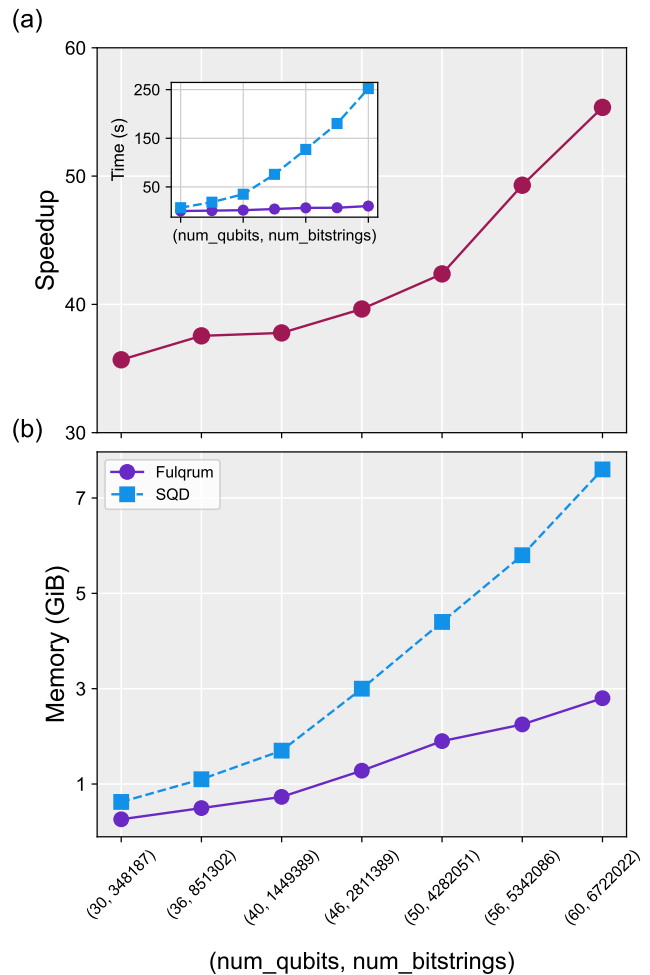


FIG. 1. (a) Ratio of `qiskit-addon-sqd` (SQD) to FULQRUM runtimes for projecting a 1D Heisenberg spin chain Hamiltonian over subspaces defined by post-processed bit-strings sampled from the IBM Marrakesh device for differing numbers of qubits running on Computer A. Inset shows time to solution for the full ground state eigenproblem of the same Hamiltonians and subspaces using SQD (squares-dashed) and FULQRUM (circles-solid). The lowest of five runs is used for timing. (b) Peak memory consumption for full eigensolutions to problems presented in (a).

of qubits and bit-strings examined by FULQRUM is over and order of magnitude faster than `qiskit-addon-sqd`, with the difference in projection timings diverging as the number of qubits and bit-strings grows; FULQRUM scales markedly better than `qiskit-addon-sqd` as problem sizes extend into the regime where quantum applications may show advantage over their classical counterparts. A similar trend is seen for the difference in timing of the full eigen workflow, inset of Fig. (1a), where, although both solvers make use of ARPACK, unlike `qiskit-addon-sqd` that uses the default serial SpMV in SCIPY, FULQRUM wraps its SpMV implementation in a `CSRLinearOperator` [see Sec. (III C)] allowing for processing matrix rows in parallel using OPENMP. Finally, the difference between the peak memory consumption of the two implementations also widens with subspace dimension and number of qubits, allowing FULQRUM to solve larger problem instances given fixed memory resources. Note that, while we could also use a matrix-free solution, the memory size of the resultant matrix is much smaller than that needed to store the subspace information, and thus is it not practical to do so.

For fermionic Hamiltonians, we select two molecular Hamiltonians. First is the N_2 molecule in the cc-pvdz basis [34], and the second is a methane (CH_4) dimer in aug-cc-pVQZ basis [35]. For the N_2 molecule, we generate bit-strings by running the corresponding chemistry-specific Local Unitary Cluster Jastrow (LUCJ) [36] quantum circuit on the IBM Boston 156-qubit Heron quantum processor sampling the circuit one million times. Out of these samples, 3,722 are bit-strings generated with the correct electron number in each electron sector. To correct the remaining bit-strings we run one round of configuration recovery to generate bit-strings with physically valid numbers of electrons [13]. The full corrected set of bit-string is split into alpha (spin up) and beta (spin down) halves and curated together with duplicates removed. Finally, 6,000 half bit-strings from this collection are selected to span the final subspace of 36 million full bit-strings by taking the Cartesian product. The sampled quantum subspace for the CH_4 dimer is comprised of configuration recovered bit-strings taken from Ref. [35]. Detailed molecular information, subspace dimensions, and computed electronic energies for the sampled subspaces are given in Tbl. (I). Note that the product of the subspace dimension and the number of groups equals the number of matrix-element evaluations that needs to be performed. However, When confined to a subspace, it does not equal the number of elements in the resultant Hamiltonian matrix.

While configuration recovery corrected bit-strings obey the correct particle number statistics, this procedure does not guarantee that the resultant subspace has strong overlap with ground state bit-strings of appreciable amplitude; this procedure can generate subspaces with superfluous bit-strings that have little to no impact on the eigensolution. On present day quantum hardware, the impact of noise is such that only a small fraction of bit-

Parameter name	N_2	CH_4 dimer
Num. (spatial) orbitals	26	24
Num. electrons (α/β)	10 (5/5)	16 (8/8)
Subspace dimension	36,000,000	65,983,129
RAMPS trimming tol.	1×10^{-14}	1×10^{-12}
RAMPS subspace dim.	751,241	1,701
Num. groups (FULQRUM)	16,073	30,105
FULQRUM operator trimming tol.	-	3×10^{-7}
Num. groups after trimming	-	13,429
Est. electronic energy (Ha.)	-32.89242	-44.05140

TABLE I. Parameters defining the N_2 and CH_4 -dimer quantum chemistry problems considered in this work. The number of qubits in the qubit Hamiltonian generated by the extended JW transformation is twice the number of orbitals.

strings (e.g. $\sim 10^{-3}$ for the N_2 subspace) are uncorrupted, thus requiring large subspaces for producing accurate results. As such, in addition to the original subspaces, we will use a recursive algorithm for minimal perturbative subspaces (RAMPS), that prunes the subspace to only those bit-strings that impact the final eigenenergy up to a user supplied tolerance value. This procedure, a pre-processing step not directly related to the framework presented here, is outlined in Supplemental Material.

We solve both molecules using FULQRUM and the popular chemistry package DICE [28, 37] on Computer B, comparing time-to-solution and peak memory consumption. As FULQRUM does not perform eigensolving itself, we are free to select the Hermitian eigensolver PRIMME [24] utilizing the `PRIMME_LOBPCG_OrthoBasis` method, which is PRIMME’s implementation of Locally Optimal Block Preconditioned Conjugate Gradient (LOBPCG) algorithm [38]. We select an initial trial vector that is peaked at the index corresponding to the diagonal element within the subspace with the lowest energy. In addition, we trim groups for the CH_4 dimer corresponding to matrix-elements whose ratio with the smallest diagonal energy splitting in the subspace is less than the trimming tolerance in Tbl. (I); groups that have no appreciable effect on the output eigenenergy are removed before matrix evaluation. DICE is installed using the RIKEN branch from Ref. [39] and invoked using the `solve_hci()` method from the `qiskit-addon-dice-solver` [40]. DICE is run in *selected configuration interaction* (SCI) mode that prevents the inclusion of configurations (bit-strings) outside the initial subspace by setting the maximum number of heat-bath configuration (HCI) iterations (`max_iter`) to 1 and the `select_cutoff` to the largest signed 32-bit integer value ($2^{31} - 1$).

The comparison between FULQRUM and DICE in terms of both solution time and peak memory consumption [41] are presented in Fig. (2). For FULQRUM we solve each molecule in the original subspace using the “fast” CSR matrix building mode presented in Sec. (III C) along with matrix-free evaluation, as well as in a reduced subspace found by running the RAMPS algorithm to trim the initial subspace to only those bit-strings corresponding to

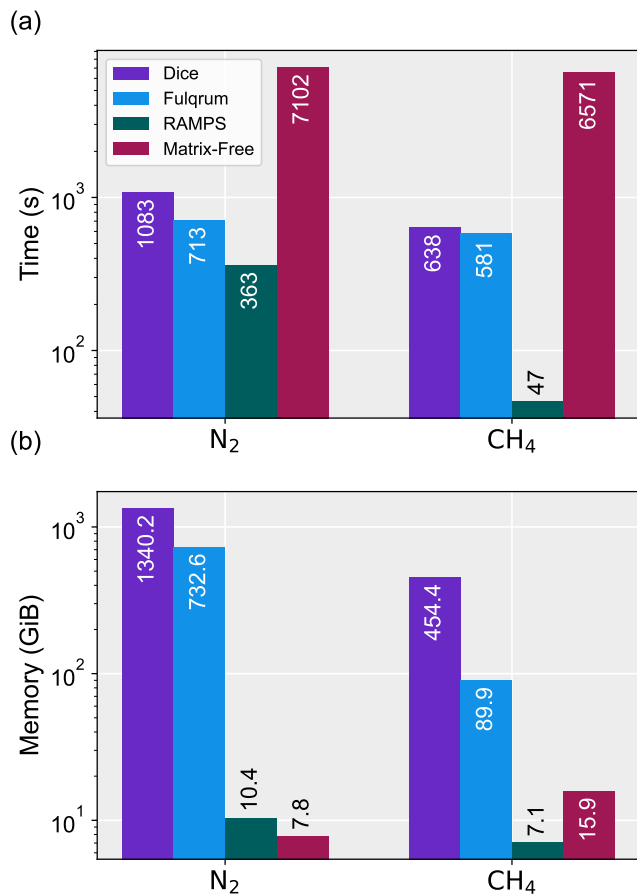


FIG. 2. (a) Time to solution for computing the ground state eigenproblem to N₂ and CH₄ dimer using DICE (purple) and FULQRUM for an initial subspace of ~ 66 million bit-strings running on Computer B. Times shown are the lowest of five runs. Both FULQRUM (blue) and RAMPS (green) solutions generate CSR matrices using the “fast” FULQRUM CSR workflow, with the latter first trimming the subspace to 1701 bit-strings before matrix evaluation. The Matrix-free (red) solution uses the full subspace dimensionality. Labels show the elapsed time rounded to the nearest second for brevity. (b) Peak memory consumption for solutions presented in (a). Labels indicate memory consumption rounded to the nearest 100 MiB.

matrix-elements that effect the resultant eigenenergy by more than the tolerance values given in Tbl. (I). Each method was configured to achieve same ground state energy given in Tbl. (I); a relative error of $\mathcal{O}(10^{-7})$. We set number of `mpirun` processes to 50 in DICE runs. To ensure fairness, we set `OMP_NUM_THREADS=50` for FULQRUM runs for all three FULQRUM modes, i.e, the full CSR matrix and matrix free modes with the original subspace and the RAMPS trimmed subspace. The RAMPS procedure was started at the subspace bit-string with lowest energy, and this energy was used as the approximate target eigenenergy, see Supplemental Material.

From Fig. (2) it is clear that FULQRUM outperforms DICE in terms of runtime and memory consumption for

both molecules. When building a CSR matrix in the full subspace, FULQRUM is 34% and 9% faster than DICE on the N₂ and CH₄ dimer, respectively. The difference in terms of memory is more pronounced, with a $\sim 2x$ reduction in peak memory compared to DICE on N₂ whereas the calculation for CH₄, aided by dropping negligible groups, demonstrates a full 5x decrease in required memory.

The RAMPS routine in FULQRUM further cuts down peak memory and accelerates time-to-solution by trimming the subspace bit-strings; RAMPS reduces the dimensionality of the resultant matrix and thus number of nonzero elements that need to be computed. In these examples, the subspace dimensionality for N₂ is cut down by 40x, where as the CH₄ dimer subspace sees a 39,000x reduction. Utilizing the RAMPS trimmed subspace, FULQRUM consumes an order of magnitude less memory than the full subspace solutions, and up to $\sim 130x$ less than DICE on N₂. Note that we use two different RAMPS trimming tolerance values [see Tbl. (I)] for the molecules so that the RAMPS energies match those of the full subspace FULQRUM and DICE runs to the prescribed accuracy. The RAMPS algorithm used here runs in serial, and further reductions in runtime can be gained by evaluating bit-strings in parallel.

As the matrix-free mode of FULQRUM does not explicitly store a matrix, it consumes significantly lower peak memory for the original subspace, albeit trading off time to solution. As seen in Fig. (2), matrix-free mode consumes $\sim 94x$ and $\sim 172x$ less memory than FULQRUM’s CSR matrix-based method and DICE, respectively, for the N₂ molecule, making it feasible to run full subspace calculations on a personal laptop. For the CH₄ dimer, memory reductions are $\sim 6x$ and $\sim 28x$ for FULQRUM and DICE. Note that matrix-free evaluation does not reduce the memory requirement for storing the subspace. Matrix-free mode is however necessarily slower due to the repeated evaluation of matrix elements. It takes $\sim 10x$ and $\sim 6.5x$ longer than FULQRUM and DICE, respectively, for N₂, while being $\sim 11x$ and $\sim 10x$ slower for CH₄. This time-memory tradeoff is nominally reserved for those problems where explicit matrix construction is not a viable option due to strict memory limitations.

II. DISCUSSION

We have demonstrated a unified solution method for eigenproblems to qubit and fermionic systems with no inherent limit on the number of qubits, and performance that is better than widely used frameworks in terms of both time-to-solution and memory consumption. This is aided by the flexibility inherent in framework, where users are free to select their classical eigensolver of choice that, along with methods such as matrix-free evaluation and the RAMPS procedure introduced here, can further optimize the performance of specific problem instances. In addition to showing that QSD problems can be faith-

fully computed with modest computing requirements, our FULQRUM package is easily installed using standard PYTHON packaging tools, further reducing the barrier to entry, as compared to tools such as DICE.

As with any piece of software, the performance of the initial version of FULQRUM presented here can likely be improved upon in several ways. To begin, Message-passing (MPI) support should to be implemented, and FULQRUM needs to move from a hybrid framework leveraging CYTHON to a C++ centric code base. The latter would allow for in-depth profiling for bottlenecks. In addition, the performance of FULQRUM compared to other tools degrades as the number of groups increases. This suggests further opportunities for optimizing group handling, such as bulk rejection of groups, likely exist. The ordering of groups within the full Hamiltonian also plays a role in cache alignment, a topic we have yet to explore. Moreover, our subspace refinement algorithm, RAMPS, is currently limited by its serial implementation and parallel evaluation of row bit-strings should be added to make the routine practical at large dimensions.

Finally, and perhaps most importantly, understanding how to optimize workflows that include subspace refinement methods, such as the RAMPS technique presented here, will help to better address the question as to whether QSD applications may offer a viable pathway to near-term Quantum Advantage. We hope that FULQRUM, or a community-based derivative, can help to answer this in the affirmative.

III. METHODS

Here we give a detailed description of the implementation of FULQRUM. Our method is primarily written in C++17 with parallelism provided by OPENMP and PYTHON bindings utilizing CYTHON [44] that take advantage of both NUMPY [45] and SCIPY [33].

The canonical FULQRUM workflow is presented in Fig. (3) where it is shown that the role of FULQRUM is to take bit-strings sampled from a quantum processor representing the subspace of interest, together with the operator representation of a system Hamiltonian, and produce SpMV-compatible numerical data structures that can be passed to a wide range of eigensolvers. This procedure can be partitioned into three primary components: Hamiltonian representations, subspace data structure, and matrix evaluation.

A. Hamiltonian representations

1. Qubit Hamiltonians

Our goal is to build numerical representations compatible with SpMV, e.g. Compressed Sparse Row (CSR) matrices or matrix-free methods, from qubit Hamiltonians that are expressed as linear combinations of terms,

each comprised of a word of qubit operators \hat{W}_i together with a complex-valued coefficient c_i : $\hat{H} = \sum_i c_i \hat{W}_i$. Nominally, the alphabet in which words are expressed is the Pauli operators \hat{I} , \hat{Z} , \hat{X} , and \hat{Y} , that are valid for execution on a quantum computer. However, because we perform eigensolving classically, we are free to work with an *extended alphabet* that includes projection operators $\hat{0}$, and $\hat{1}$, together with the ladder operators \hat{a}^- and \hat{a}^+ . In what follows we drop the identity operator as it plays a trivial role in calculations; terms are represented using a sparse encoding. Internally each term is represented as an `OperatorTerm` with complex-valued coefficient together with two vectors, one indicating the indices on which individual non-identity operators act, sorted in ascending order, and a vector of characters labeling the operators themselves. We use the mapping $[Z, 0, 1, X, Y, -, +] \rightarrow [0, 1, 2, 3, 4, 5, 6]$, where off-diagonal operators correspond to values > 2 . The `QubitOperator` class stores the vector of terms corresponding to a full Hamiltonian H .

Of particular importance for matrix evaluation are the qubit indices on which the off-diagonal operators of a term, if any, act. We will call this set of indices the *off-diagonal structure* as it plays an outsized role in efficiently computing matrix-elements. Restricting ourselves to Pauli-words, the following hold true for terms in a Hamiltonian described over a subspace of the computational basis represented by bit-strings:

1. For a given bit-string from the subspace representing a row in the Hamiltonian matrix, there exists exactly one nonzero element per term; The matrix representation of a term in the subspace has a single nonzero entry per row [46].
2. The bit-string for the column corresponding to the nonzero element from (1) is found by flipping the bits of the row bit-string at the off-diagonal structure indices; the off-diagonal indices give a bit-mask that XOR with the row bit-string to yield the column bit-string.
3. As a corollary to (2), terms that share the same off-diagonal structure correspond to the same matrix-elements.

While there is a guaranteed nonzero element per row bit-string for a term comprised of a Pauli-word, the column bit-string corresponding to that value need not live within the selected subspace. It is therefore necessary to query the subspace as to whether a given column is a member or not. Asking this question is computationally expensive and requires judicious selection of data structures for the subspace to yield acceptable performance, see Sec. (IIIB). However, item (3) tells us that such "column lookups" are not needed for every term but rather can be done once per *group* of terms that have matching off-diagonal structure. To partition a Hamiltonian into these groups we first sort terms by their off-diagonal

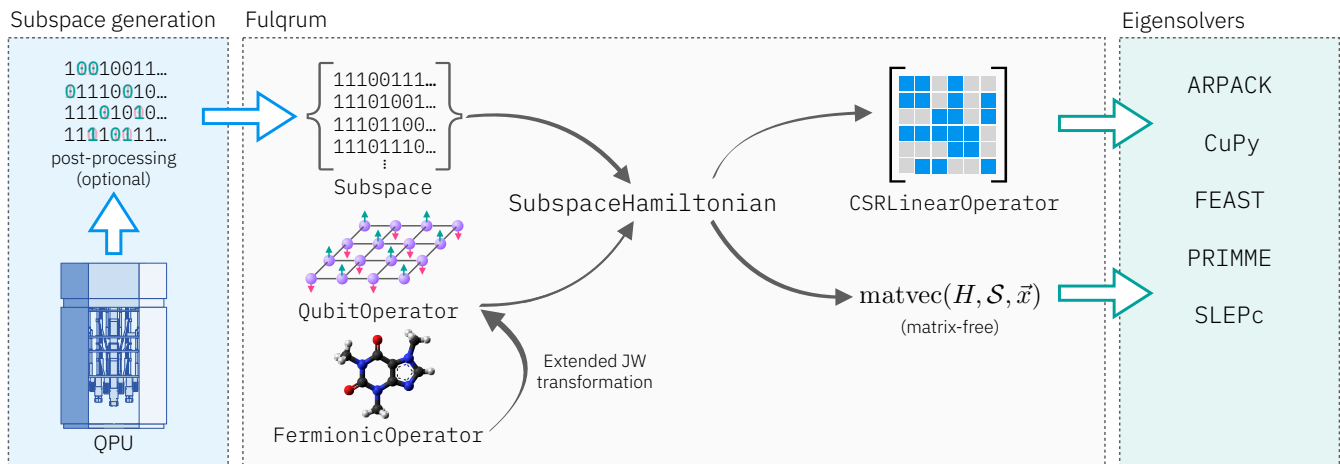


FIG. 3. Exemplar FULQRUM workflow. Bit-strings sampled from a quantum processing unit (QPU), with optional post-processing such as SQD, are used to construct a **Subspace** instance that, together with a corresponding qubit (**QubitOperator**) or fermionic (**FermionicOperator**) Hamiltonian representation, are used to build a **SubspaceHamiltonian** model. Fermionic systems are cast to equivalent qubit representations via an extended-alphabet JW transformation for a unified solution method. From a **SubspaceHamiltonian**, users can generate CSR-matrix representations (**CSRLinearOperator**), or utilize matrix-free solution methods via the abstract **LinearOperator** class (**matvec**) in SciPy, passing these on to a wide range of classical eigensolvers [23–25, 42, 43].

weight, i.e. the number of off-diagonal single-qubit operators in a term, and then collect terms that share off-diagonal structure in parallel over subsets of matching off-diagonal weight. Each group can then be given an integer index. Terms with zero off-diagonal weight are diagonal components of the Hamiltonian and represent a single group. At the output of this procedure is a Hamiltonian with terms organized into groups together with an array of pointers, (**group_ptrs**), that gives the start and stop indices of the terms, with respect to the full Hamiltonian, that correspond to each group. An example of this procedure is shown in Fig. (4).

Terms expressed over the full extended alphabet follow the same set of rules with the caveat that the single matrix-element per row can be zero if the term is comprised of one or more projector and/or ladder operators. Such operators place constraints on the bit-values at the corresponding operator indices for which nonzero values occur. For a word with m projection or ladder operators, the fraction of rows with nonzero entries is reduced to $1/2^m$. Although qubit Hamiltonians are nominally not expressed using these extended operators, as discussed in the subsequent section, fermionic systems naturally utilize these operators, and we can leverage these constraints to greatly reduce the number of terms that need to be computed for matrix evaluation.

2. Fermionic Hamiltonians

Fermionic systems differ from those of qubit Hamiltonians in two important ways. First is the use of fermionic ladder operators, f^\dagger and f , that obey the

canonical anti-commutation relations: $\{f_i, f_j\} = 0$ and $\{f_i, f_j^\dagger\} = \delta_{ij}$. And second is the possibility of having multiple operators act on the same mode index. Despite these differences, it is beneficial to represent fermionic terms (**FermionicTerm**) and Hamiltonians (**FermionicOperator**) using the same data structures as qubit Hamiltonians. Likewise, we sort indices in ascending order, keeping track of sign changes when exchanging operators on different indices. In addition, we merge operators acting on repeated indices within a term according to the rules in Supplemental Material, which yields an operator comprised of both ladder operators and projectors. While it is possible to directly build fermionic operators in FULQRUM, standard workflows involve converting fermionic operators from tools such as OPENFERMION [47] or QISKIT NATURE [48] into their equivalent FULQRUM representations.

As we aim to have a unified solution method, we transform fermionic operators into qubit operators via a Jordan-Wigner (JW) transformation [31]. In contrast to the standard JW transformation, we do not decompose fermionic ladder operators into Pauli operators, $f_j = \frac{1}{2}(X_j + iP_j)Z_{j-1} \otimes \cdots \otimes Z_0$, and instead directly map projection and ladder operators into their qubit counterparts along with adding the Z operators needed to maintain commutation relations. An important step in this transformation is the combining of repeat terms with differing coefficients that are usually generated in fermionic Hamiltonians, and this operation takes the majority of the time in the transformation. To improve performance, at the end of the JW transformation itself we sort terms in the output **QubitOperator** by their weight, i.e. the total number of non-identity single-qubit opera-

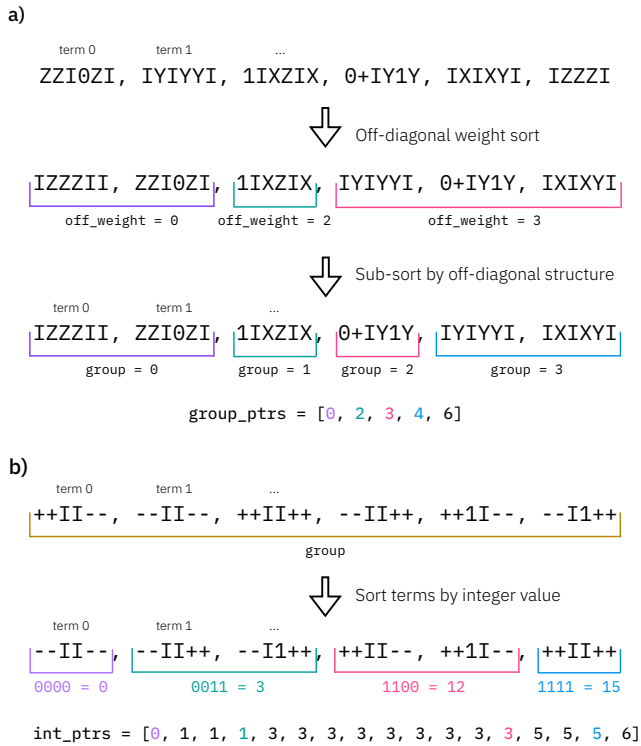


FIG. 4. Term sorting methods used in FULQRUM. a) Groups of terms corresponding to matrix elements are sorted into contiguous order by first ordering all terms by their off-diagonal weight, and then sub-sorting terms with matching off-diagonal weight by their off-diagonal structure. Both steps can be done in parallel. The starting and stopping term indices for each group are stored in the group pointers array. b) Sorting by integer value within a group comprised from terms with off-diagonal structure determined by ladder operators.

tors, and combine terms within each subset of constant weight in parallel to significantly speed up the computation. An example is shown in Tbl. (II), where the total JW transformation time is markedly faster than existing frameworks with similar functionality. With this time being a small fraction of the overall eigensolving runtime for fermionic systems, requiring this transformation in order to have a unified solution method does not represent a

Framework	Time (sec)
CUDA-QX (0.5.0)	282
FULQRUM	0.51
OPENFERMION (1.7.1)	51
PENNYLANE (0.44.0)	980
PYCHEMIQ (1.4.1)	40
QISKIT-NATURE (0.7.2)	78
QRISP (0.7.17)	57

TABLE II. Time taken by Computer A to compute the Jordan-Wigner transformation for H₂O in the cc-pvdz basis generated by PYSCF for this work along with a selection of software packages with similar functionality [47–52].

bottleneck in our method.

At the output of the JW transformation the resulting qubit Hamiltonian is expressed with operators in the set $\{Z, 0, 1, -, +\}$, with the off-diagonal structure determined solely by ladder operators. As stated in Sec. (III A 1), these extended operators constrain the possible bit-values for which a row bit-string yields a nonzero value for a given term. We can leverage this on a group by group basis by converting the ladder operators in each term to the binary representation of an integer with the mapping $- \rightarrow 0, + \rightarrow 1$; a value we call the terms *ladder integer*. The terms within the group are then sorted in ascending order according to these ladder integer values. Associated with each group is an array of pointer values (`int_ptrs`) that records the starting and stopping indices, with respect to the full Hamiltonian, of terms within the group that have a given ladder integer value. Molecular electronic Hamiltonians can be written in the form

$$H = H_0 + \sum_{p,q} h_{p,q} f_p^+ f_q + \frac{1}{2} \sum_{p,q,r,s} f_p^+ f_q^+ f_r f_s$$

where H_0 is a constant offset nuclear repulsion energy and $h_{p,q}$ and $h_{p,q,r,s}$ are one- and two-body integrals, respectively [53], showing that at most four ladder operators are present in a term. We therefore need a pointer array of size $2^4 + 1$ to accommodate all possible ladder integer values. An example is given in Fig. (4b). For each off-diagonal group in the Hamiltonian we compute the ladder integer for a given row bit-string using the indices comprising the off-diagonal structure for the group. Only those terms in the group that have a matching ladder integer value give a nonzero contribution to the resultant matrix-element, assuming the column bit-string is also in the subspace. While this reduces the number of terms that need to be numerically evaluated, the primary savings come from those groups where no term shares the row bit-string ladder integer value; there is no column lookup, or any other processing, for the group as the matrix-element is zero. In practice, this leads to a $\sim 10x$ decrease in the runtime for matrix construction of fermionic systems

B. Subspace data structure

The `Subspace` in FULQRUM is a collection of bit-sets [54], `boost::dynamic_bitset<size_t>`, defining the rows and columns of a Hamiltonian matrix. FULQRUM's algorithm requires both insertion order indexing and fast lookup operations, and therefore the choice of subspace data structure is paramount for performance and memory-efficiency. A key routine in FULQRUM is fetching a row bit-set by index and constructing a potential column bit-set by flipping bits at the indices specified by the off-diagonal structure in the row bit-set. We then lookup the candidate column bit-set in the subspace. If it the bit-set is in the subspace, the matrix element between that

row and column needs to be evaluated. Because we filter out nonzero values *before* querying the subspace, this element value is nonzero, and should be included in the output matrix, or computed for matrix-free SpMV. To ensure sufficient performance, we need a data-structure that allows for fetching multiple (row) bit-sets in parallel, and that also offers fast search capabilities. Here we use `emhash8::HashMap` [55] to store and look up bit-sets as it provides both features, and `rapidhash` [56] as the bit-set hasher.

Most C++ hash maps, including `std::unordered_map`, do not allow parallel iteration over keys. Had we chosen a different hash map, we would need a vector to store bit-sets and to allow for parallel iteration, whilst also maintaining the hash map for fast look up. Having two data structures to store identical information would necessarily increase the memory footprint of FULQRUM. `emhash8::HashMap` allows for indexed-access to key-value pairs in insertion order, similar to a `std::vector`. We can therefore parallelize the access to keys using, e.g., using `OpenMP`, thus achieving both parallelism and fast look up in a single data structure.

`emhash8::HashMap` stores key-value pairs in *buckets*. During a key look up, it follows a standard hash map look up routine where the key is first hashed and then a hash value, modulo the number of buckets, is performed to find a potential bucket index where the key might be stored. If the bucket at that index is *empty*, the key is guaranteed not to be in the hash map. To improve search performance, we edited the `emhash8::HashMap` implementation to include a variable to store the bucket occupancy information. The variable is a `boost::dynamic_bitset<size_t>` with a width (number of bits) equal to the number of buckets. Initially, all bits are off in this bit-set, indicating empty buckets. When we put a key-value pair in a bucket during insertion, the corresponding bit will be set to on. During search, we first inspect this bucket occupancy bit-set to validate the bucket is occupied before looking into the main bucket structure. If the bit is off, the bucket is empty and the search terminates yielding a faster way to reject empty buckets. For example, for a 64 bytes cache-line load, the bit-set-based implementation can bring occupancy information about $64 \times 8 = 512$ bits (buckets) in the cache, improving the cache hit rate. Had we directly queried main bucket structure, which has at least two `size_t` (2×8 bytes) items per bucket, a single cache-line load, theoretically, only brings $64 / (2 \times 8) = 4$ buckets in the cache. Note that we can leverage this faster empty bucket test because we know the number of key-value pairs in our hash map a priori. This allows for reserving storage space and fixing the total number of buckets in the hash map, ultimately informing us of the number of required bits in the bit-set. Moreover, we can reserve more capacity in the hash map than necessary to keep the hash map load factor low. A lower load factor improves search performance, especially for missing items, as we can reject empty buckets faster using our modification.

C. Matrix evaluation

Numerical representations of a subspace Hamiltonian are generated by first combining a `Subspace`, `S`, and `QubitOperator` into a single `SubspaceHamiltonian` class. Within this object the Hamiltonian is split into diagonal and off-diagonal components, with the diagonal matrix elements within the subspace being computed in parallel and cached. This calculation is accelerated when working over terms with projection operators, such as those for fermionic systems, where it is possible to efficiently pass-over null terms based on bit-values of the row bit-string at the projector operator indices. In practice, this yields a $\sim 20\%$ reduction in diagonal build time. Off-diagonal Hamiltonian terms are sorted into groups, and if the Hamiltonian is derived from a fermionic system, groups are further sorted by their terms ladder operator (off-diagonal structure) derived integer values.

The primary output format for a subspace Hamiltonian is a CSR sparse matrix, selected for its wide-compatibility with classical eigensolving frameworks. It is possible to build a CSR matrix directly, with no intermediate copies, using a two-pass method where the first pass computes the number of nonzero entries per row of the Hamiltonian (the sparse structure) while the second pass populates the matrix element values. Both stages proceed by independently iterating over the bit-strings of a subspace in parallel, with each bit-string representing a row of the CSR matrix. The cached diagonal elements are processed first, while the off-diagonal Hamiltonian is treated group-by-group. For a given row-bit-string we only evaluate those groups with matrix-elements in the lower-triangle, see Sec. III C 1 for further details. If the Hamiltonian is derived from a fermionic system then the ladder integer value for the bit-string determined by the off-diagonal structure for the group is computed and used to index the `int_ptrs` corresponding to the group which sets the start and stop indices used to loop over nonzero terms in the group. If there are no matching ladder integer terms in the group then the start and stop indices are identical and the group is skipped.

For groups with nonzero terms, we first compute the corresponding column bit-string for the matrix-element using the off-diagonal structure, and perform a hash map lookup to determine if this column bit-string is within the subspace. If so, then the relevant terms within the subspace, i.e. all terms for spin Hamiltonians and those with ladder integer values that match the row bit-string for fermionic systems, are further refined by considering the value of bits at the location of projection operators, if any, to further identify zero terms. At the end of this process, only terms with nonzero contribution to the matrix-element are numerically evaluated and summed.

If computing the sparse structure (first pass), the number of nonzero elements per matrix row are stored in array, `indptr`, of length $\dim(\mathcal{S}) + 1$, with the last element representing the total number of nonzero elements (NNZ) in the matrix. The second pass uses structure in-

formation from pass one to construct arrays of column indices (`indices`) and matrix-element values (`data`), both of length `NNZ`, and populates them by processing the matrix again. The trinity (`indptr`, `indices`, `data`) is used to build a `SCIPY csr_matrix` that is then wrapped in a `CSRLinearOperator` that allows overloading the `CSR SpMV` operation to allow for `OPENMP` parallelization. `FULQRUM` automatically uses the smallest data-types for both the matrix data (`double` or `double complex`) and row and column indices (`int32` or `int64`) both internally and for the output `CSR` matrix.

While the two-pass method allows for direct `CSR` construction with no copies, it is computationally expensive to evaluate matrix-elements twice. As such, we introduce a “fast” `CSR` construction method that utilizes an array of $\dim(S)$ objects comprised of dynamically allocated `C++` vectors for column indices and matrix-element values to populate a data structure similar to `CSR` format in a single step. While `SpMV` operations with this data structure are $\sim 3x$ slower than using `CSR` format, it is efficient to convert to standard `CSR` format at the expense of a data copy. In practice, this time / memory tradeoff is often acceptable, and this fast `CSR` construction is the preferred method in `FULQRUM`.

In situations where memory constraints make explicit matrix storage impractical, it is possible to perform the `SpMV` operations required for sparse eigensolving using matrix-free methods. However, these techniques do not alleviate the memory requirements for storing the subspace and Hamiltonian. In `FULQRUM`, the `SubspaceHamiltonian` is a subclass of the `SCIPY LinearOperator` class and, replacing a matrix, can be directly passed to eigensolvers supporting this format for matrix-free evaluation, e.g. [24, 33], and with work [57], also [25]. Given in input vector, `SpMV` computation is performed in parallel over row bit-strings in a similar manner as `CSR` matrix construction, where the action of each row bit-string on the input vector is used to populate the value of the output vector at same row index. Because no data are stored between runs, each `SpMV` call requires recomputing matrix-elements; each matrix-free `SpMV` call is comparable to fast `CSR` matrix construction in terms of runtime. As such, the number of iterations performed by the eigensolver dictates the overall runtime of our matrix-free algorithm. It is therefore most useful when teamed with a good initial trial vector and utilized for low-precision solutions, or no other method is feasible due to memory constraints.

1. Lower / upper triangle evaluation

As we are working with Hermitian matrices, it is possible to completely characterize the Hamiltonian matrix using matrix-elements in the the upper or lower triangle only. We can exploit this opportunity to cut down

the number of matrix element evaluations by half, possibly speeding up `CSR` matrix build time by $\sim 2x$. While this is conceptually straightforward, there are implementation challenges in direct implementation. Importantly, we need an efficient way to determine if a matrix-element is in the upper or lower triangle. Focusing on the lower-triangle, for an element to be in the lower triangle, the index of a row bit-string must be greater than the index for the associated column bit-string for a given group. Although we can compute the column bit-set first and perform a column lookup, the cost of doing so offsets any gains from looking at the lower or upper triangle only. To get around this, we first sort subspace bit-strings by their integer values. This takes only a small fraction of time with respect to the overall eigensolution runtime, and can be performed in parallel. We can then determine if the matrix-element for a given group is within the lower triangle by inspecting the row bit at largest index in the groups off-diagonal structure; the *most-significant off-diagonal bit* (`MJOB`). If the bit at the `MJOB` position of a row bit-string is on, then it will be flipped to off when computing the column bit-string, and the integer sorting of the subspace bit-strings guarantees that the matrix-element is in the lower-triangle of the Hamiltonian. Similarly, if the `MJOB` row bit is off then the corresponding bit in the column bit-set will be on, and we know the element is in the upper-triangle. In this way, we are able to compute only lower/upper triangle matrix-elements without computing the column bit-string itself. Examples of this method are given in Supplemental Material.

ACKNOWLEDGMENTS

The authors thank Jim Garrison for helpful discussions and Danil Kaliakin, Zhen Li, and Kenneth Merz for permission to use CH_4 dimer bit-strings and operator representation from Ref. [35].

AUTHOR CONTRIBUTIONS

`PDN` conceived the project, derived the operator grouping and extended alphabet methods, developed the `RAMPS` procedure, and wrote the initial code base. `AAS` developed the optimized hash map routines, created the method of efficient upper / lower triangle evaluation along with better group rejection logic, ran the fermionic system examples, and contributed to the overall performance of the framework. `HK` implemented and ran the `SKQD` workflow experiments, as well as helped derive the extended operator functionality and `RAMPS`. All authors contributed to the manuscript.

-
- [1] K. Bharti, A. Cervera-Lierta, T. H. Kyaw, T. Haug, S. Alperin-Lea, A. Anand, M. Degroote, H. Heimonen, J. S. Kottmann, T. Menke, W.-K. Mok, S. Sim, L.-C. Kwek, and A. Aspuru-Guzik, Noisy intermediate-scale quantum algorithms, *Rev. Mod. Phys.* **94**, 015004 (2022).
- [2] M. Cerezo, A. Arrasmith, R. Babbush, S. C. Benjamin, S. Endo, K. Fujii, J. R. McClean, K. Mitarai, X. Yuan, L. Cincio, and P. J. Coles, Variational quantum algorithms, *Nat. Rev. Phys.* **3**, 625 (2021).
- [3] A. Y. Kitaev, Quantum measurements and the Abelian Stabilizer Problem, arXiv:quant-ph/9511026 [10.48550/arXiv.quant-ph/9511026](https://arxiv.org/abs/10.48550/arXiv.quant-ph/9511026) (1995).
- [4] D. S. Abrams and S. Lloyd, Quantum Algorithm Providing Exponential Speed Increase for Finding Eigenvalues and Eigenvectors, *Phys. Rev. Lett.* **83**, 5162 (1999).
- [5] D. Poulin and P. Wocjan, Preparing Ground States of Quantum Many-Body Systems on a Quantum Computer, *Phys. Rev. Lett.* **102**, 130503 (2009).
- [6] Y. Dong, L. Lin, and Y. Tong, Ground-State Preparation and Energy Estimation on Early Fault-Tolerant Quantum Computers via Quantum Eigenvalue Transformation of Unitary Matrices, *PRX Quantum* **3**, 040305 (2022).
- [7] Y. Alexeev, V. S. Batista, N. Bauman, L. Bertels, D. Claudino, R. Dutta, L. Gagliardi, S. Godwin, N. Govind, M. Head-Gordon, M. R. Hermes, K. Kowalski, A. Li, C. Liu, J. Liu, P. Liu, J. M. Garcia-Lastra, D. Mejia-Rodriguez, K. Mueller, M. Otten, B. Peng, M. Raugas, M. Reiher, P. Rigor, W. J. Shaw, M. v. Schilfhaarde, T. Vegge, Y. Zhang, M. Zheng, and L. Zhu, A Perspective on Quantum Computing Applications in Quantum Chemistry Using 25–100 Logical Qubits, *J. Chem. Theory Comput.* **21**, 11335 (2025).
- [8] S. McArdle, S. Endo, A. Aspuru-Guzik, S. C. Benjamin, and X. Yuan, Quantum computational chemistry, *Rev. Mod. Phys.* **92**, 015003 (2020).
- [9] H. Zhang and M. Otten, Subspace methods for electronic structure simulations on quantum computers, arXiv:2313.00178 [10.48550/arXiv.2312.00178](https://arxiv.org/abs/10.48550/arXiv.2312.00178) (2023).
- [10] A. Abbas, A. Ambainis, B. Augustino, A. Bärttschi, H. Buhrman, C. Coffrin, G. Cortiana, V. Dunjko, D. J. Egger, B. G. Elmegreen, N. Franco, F. Fratini, B. Fuller, J. Gacon, C. Gonciulea, S. Gribling, S. Gupta, S. Hadfield, R. Heese, G. Kircher, T. Kleinert, T. Koch, G. Korpas, S. Lenk, J. Marecek, V. Markov, G. Mazzola, S. Mensa, N. Mohseni, G. Nannicini, C. O’Meara, E. P. Tapia, S. Pokutta, M. Proissl, P. Rebentrost, E. Sahin, B. C. B. Symons, S. Tornow, V. Valls, S. Woerner, M. L. Wolf-Bauwens, J. Yard, S. Yarkoni, D. Zechiel, S. Zhuk, and C. Zoufal, Challenges and opportunities in quantum optimization, *Nature Reviews Physics* **6**, 718 (2024).
- [11] K. Kanno, M. Kohda, R. Imai, S. Koh, K. Mitarai, W. Mizukami, and Y. O. Nakagawa, Quantum-Selected Configuration Interaction: classical diagonalization of Hamiltonians in subspaces selected by quantum computers, arXiv:2302.11320 [10.48550/arXiv.2302.11320](https://arxiv.org/abs/10.48550/arXiv.2302.11320) (2023).
- [12] Y. O. Nakagawa, M. Kamoshita, W. Mizukami, S. Sudo, and Y.-y. Ohnishi, ADAPT-QSCI: Adaptive Construction of an Input State for Quantum-Selected Configuration Interaction, *J. Chem. Theory Comput.* **20**, 10817 (2024).
- [13] J. Robledo-Moreno, M. Motta, H. Haas, A. Javadi-Abhari, P. Jurcevic, W. Kirby, S. Martiel, K. Sharma, S. Sharma, T. Shirakawa, I. Sitdikov, R.-Y. Sun, K. J. Sung, M. Takita, M. C. Tran, S. Yunoki, and A. Mezzacapo, Chemistry Beyond Exact Solutions on a Quantum-Centric Supercomputer, arXiv:2405.05068 [10.48550/arXiv.2405.05068](https://arxiv.org/abs/10.48550/arXiv.2405.05068) (2024).
- [14] K. Sugisaki, S. Kanno, T. Itoko, R. Sakuma, and N. Yamamoto, Hamiltonian simulation-based quantum-selected configuration interaction for large-scale electronic structure calculations with a quantum computer, arXiv:2412.07218 [10.48550/arXiv.2412.07218](https://arxiv.org/abs/10.48550/arXiv.2412.07218) (2024).
- [15] A. Pellow-Jarman, S. McFarthing, D. H. Kang, P. Yoo, E. E. Elala, R. Pellow-Jarman, P. M. Nakliang, J. Kim, and J.-K. K. Rhee, HIVQE: Handover Iterative Variational Quantum Eigensolver for Efficient Quantum Chemistry Calculations, arXiv:2503.06292 [10.48550/arXiv.2503.06292](https://arxiv.org/abs/10.48550/arXiv.2503.06292) (2025).
- [16] J. Yu, J. Robledo-Moreno, J. T. Iosue, L. Bertels, D. Claudino, B. Fuller, P. Groszkowski, T. S. Humble, P. Jurcevic, W. Kirby, T. A. Maier, M. Motta, B. Pokharel, A. Seif, A. Shehata, K. J. Sung, M. C. Tran, V. Tripathi, A. Mezzacapo, and K. Sharma, Quantum-Centric Algorithm for Sample-Based Krylov Diagonalization, arXiv:2501.09702 [10.48550/arXiv.2501.09702](https://arxiv.org/abs/10.48550/arXiv.2501.09702) (2025).
- [17] T. Smith, T. P. Gujarati, M. Motta, B. Link, I. Liepuoniute, T. Friedhoff, H. Nishimura, N. Nguyen, K. S. Williams, J. R. Moreno, C. Johnson, K. J. Sung, A. A. Saki, and M. Kagele, Quantum-centric simulation of hydrogen abstraction by sample-based quantum diagonalization and entanglement forging, arXiv:2508.08229 [10.48550/arXiv.2508.08229](https://arxiv.org/abs/10.48550/arXiv.2508.08229) (2025).
- [18] M. A. Barroca, T. Gujarati, V. Sharma, R. Neumann, B. Ferreira, Y.-H. Na, M. Giammona, A. Mezzacapo, B. Wunsch, and M. Steiner, Surface Reaction Simulations for Battery Materials through Sample-Based Quantum Diagonalization and Local Embedding, arXiv:2503.10923 [10.48550/arXiv.2503.10923](https://arxiv.org/abs/10.48550/arXiv.2503.10923) (2025).
- [19] S. Barison, J. R. Moreno, and M. Motta, Quantum-centric computation of molecular excited states with extended sample-based quantum diagonalization, *Quantum Sci. Technol.* **10**, 025034 (2025).
- [20] D. Danilov, J. Robledo-Moreno, K. J. Sung, M. Motta, and J. Shee, Enhancing the accuracy and efficiency of sample-based quantum diagonalization with phaseless auxiliary-field quantum Monte Carlo, arXiv:2503.05967 [10.48550/arXiv.2503.05967](https://arxiv.org/abs/10.48550/arXiv.2503.05967) (2025).
- [21] T. Shirakawa, J. Robledo-Moreno, T. Itoko, V. Tripathi, K. Ueda, Y. Kawashima, L. Broers, W. Kirby, H. Pathak, H. Paik, M. Tsuji, Y. Kodama, M. Sato, C. Evangelinos, S. Seelam, R. Walkup, S. Yunoki, M. Motta, H. Jurcevic, Petar Horii, and A. Mezzacapo, Closed-loop calculations of electronic structure on a quantum processor and a classical supercomputer at full scale, arXiv:2511.00224 [10.48550/arXiv.2511.00224](https://arxiv.org/abs/10.48550/arXiv.2511.00224) (2025).
- [22] R. Bronson, *Matrix methods; an introduction* (Academic Press, New York, 1969).
- [23] R. B. Lehoucq, D. C. Sorensen, and C. Yang, *ARPACK Users’ Guide: Solution of Large-Scale Eigenvalue Problems with Implicitly Restarted Arnoldi Methods* (SIAM,

- 1987).
- [24] A. Stathopoulos and J. R. McCombs, PRIMME: Preconditioned Iterative MultiMethod Eigensolver: Methods and software description, *ACM Transactions on Mathematical Software* **37**, 21 (2010).
- [25] V. Hernandez, J. E. Roman, and V. Vidal, SLEPc: A scalable and flexible toolkit for the solution to eigenvalue problems, *ACM Trans. Math. Software* **31**, 351 (2005).
- [26] Y. Saad, *Numerical Methods for Large Eigenvalue Problems*, 2nd ed. (SIAM, 2011).
- [27] Q. Sun, X. Zhang, S. Banerjee, P. Bao, M. Barby, N. S. Blunt, N. A. Bogdanov, G. H. Booth, J. Chen, Z.-H. Cui, J. J. Ericksen, Y. Gao, S. Guo, J. Hermann, M. R. Hermes, K. Koh, P. Koval, B. Lehtola, Z. Li, J. Liu, N. Mardirossian, J. D. McClain, M. Motta, B. Mussard, R. Sayfutyarova, Elvira, M. Scheuer, H. F. Schurkus, E. T. Smith, James, C. Sun, S.-N. Sun, S. Upadhyay, L. K. Wagner, X. Wang, A. White, J. D. Whitfield, M. J. Williamson, S. Wouters, J. Yang, J. M. Yu, T. Zhu, T. C. Berkelbach, S. Sharma, A. Y. Sokolov, and G. K.-L. Chan, Recent developments in the PySCF program package, *J. Chem. Phys.* **153**, 10.1063/5.0006074 (2020).
- [28] S. Sharma, A. A. Holes, G. Jeanmairet, A. Alavi, and C. J. Umrigar, Semistochastic Heat-Bath configuration Interaction Method: Selected Configuration Interaction with Semistochastic Perturbation Theory, *J. Chem. Theory Comput.* **13**, 10.1021/acs.jctc.6b01028 (2017).
- [29] D. G. A. Smith, L. A. Burns, A. C. Simmonett, R. M. Parrish, M. C. Schieber, R. Galvelis, P. Kraus, H. Kruse, R. Di Remigio, A. Alenaizan, A. M. James, S. Lehtola, J. P. Misiewicz, M. Scheurer, R. A. Shaw, J. B. Schriber, Y. Xie, Z. L. Glick, D. A. Sirianni, J. S. O'Brien, J. M. Waldrop, A. Kumar, E. G. Hohenstein, B. P. Pritchard, B. R. Brooks, I. Schaefer, Henry F., A. Y. Sokolov, K. Patkowski, I. DePrince, A. Eugene, U. Bozkaya, R. A. King, F. A. Evangelista, J. M. Turney, T. D. Crawford, and C. D. Sherrill, PSI4 1.4: Open-source software for high-throughput quantum chemistry, *J. Chem. Theory Comput.* **152**, 10.1063/5.0006002 (2020).
- [30] A. A. Saki, S. Barison, B. Fuller, J. R. Garrison, R. Glick, Jennifer, C. Johnson, A. Mezzacapo, J. Robledo-Moreno, M. Rossmannek, P. Schweigert, I. Sitdikov, and K. J. Sung, Qiskit addon: sample-based quantum diagonalization, <https://github.com/Qiskit/qiskit-addon-sqd> (2024).
- [31] P. Jordan and E. Wigner, Über das paulische äquivalenzverbot., *Z. Physik* **47**, 631 (1928).
- [32] *Fulqrum*, github.com/qiskit-community/fulqrum (2026).
- [33] P. Virtanen, R. Gommers, T. E. Oliphant, M. Haberland, T. Reddy, D. Cournapeau, E. Burovski, P. Peterson, W. Weckesser, J. Bright, S. J. van der Walt, M. Brett, J. Wilson, K. J. Millman, N. Mayorov, A. R. J. Nelson, E. Jones, R. Kern, E. Larson, C. J. Carey, Í. Polat, Y. Feng, E. W. Moore, J. VanderPlas, D. Laxalde, J. Perktold, R. Cimrman, I. Henriksen, E. A. Quintero, C. R. Harris, A. M. Archibald, A. H. Ribeiro, F. Pedregosa, P. van Mulbregt, A. Vijaykumar, A. P. Bardelli, A. Rothberg, A. Hilboll, A. Kloeckner, A. Scopatz, A. Lee, A. Rokem, C. N. Woods, C. Fulton, C. Masson, C. Häggström, C. Fitzgerald, D. A. Nicholson, D. R. Hagen, D. V. Pasechnik, E. Olivetti, E. Martin, E. Wieser, F. Silva, F. Lenders, F. Wilhelm, G. Young, G. A. Price, G.-L. Ingold, G. E. Allen, G. R. Lee, H. Audren, I. Probst, J. P. Dietrich, J. Silterra, J. T. Webber, J. Slavič, J. Nothman, J. Buchner, J. Kulick, J. L. Schönberger, J. de Miranda Cardoso, J. Reimer, J. Harrington, J. L. C. Rodríguez, J. Nunez-Iglesias, J. Kuczynski, K. Tritz, M. Thoma, M. Newville, M. Kümmerer, M. Bolingbroke, M. Tartre, M. Pak, N. J. Smith, N. Nowaczyk, N. Shebanov, O. Pavlyk, P. A. Brodtkorb, P. Lee, R. T. McGibbon, R. Feldbauer, S. Lewis, S. Tygier, S. Sievert, S. Vigna, S. Peterson, S. More, T. Pudlik, T. Oshima, T. J. Pingel, T. P. Robitaille, T. Spura, T. R. Jones, T. Cera, T. Leslie, T. Zito, T. Krauss, U. Upadhyay, Y. O. Halchenko, Y. Vázquez-Baeza, and S. . . Contributors, Scipy 1.0: fundamental algorithms for scientific computing in python, *Nature Methods* **17**, 261 (2020).
- [34] J. Dunning, Thom H., Gaussian basis sets for use in correlated molecular calculations. I. The atoms boron through neon and hydrogen, *The Journal of Chemical Physics* **90**, 1007 (1989).
- [35] D. Kaliakin, A. Shajan, F. Liang, J. R. Moreno, Z. Li, A. Mitra, M. Motta, C. Johnson, A. A. Saki, S. Das, I. Sitdikov, A. Mezzacapo, and J. Merz, Kenneth M, Accurate quantum-centric simulations of intermolecular interactions, *Commun Phys* **8**, 396 (2025).
- [36] M. Motta, K. J. Sung, K. B. Whaley, M. Head-Gordon, and J. Shee, Bridging physical intuition and hardware efficiency for correlated electronic states: the local unitary cluster jastrow ansatz for electronic structure, *Chem. Sci.* **14**, 11213 (2023).
- [37] A. A. Holmes, N. M. Tubman, and C. J. Umrigar, Heat-bath configuration interaction: An efficient selected configuration interaction algorithm inspired by heat-bath sampling, *Journal of Chemical Theory and Computation* **12**, 3674 (2016), pMID: 27428771, <https://doi.org/10.1021/acs.jctc.6b00407>.
- [38] A. V. Knyazev, Toward the Optimal Preconditioned Eigensolver: Locally Optimal Block Preconditioned Conjugate Gradient Method, *SIAM Journal on Scientific Computing* **23**, 517 (2001).
- [39] *Dice fork*, <https://github.com/caleb-johnson/Dice> (2025).
- [40] *qiskit-addon-dice-solver*, <https://github.com/Qiskit/qiskit-addon-dice-solver> (2025).
- [41] *Memory profiler*, https://github.com/pythonprofile/rs/memory_profiler (2026).
- [42] *CuPy*, github.com/cupy/cupy/ (2025).
- [43] E. Polizzi, Density-matrix-based algorithm for solving eigenvalue problems, *Phys. Rev. B* **79**, 115112 (2009).
- [44] S. Behnel, R. Bradshaw, C. Citro, L. Dalcin, D. S. Seljebotn, and K. Smith, Cython: The Best of Both Worlds, *Computing in Science and Engineering* **13**, 31 (2011).
- [45] C. R. Harris, K. J. Millman, S. J. van der Walt, R. Gommers, P. Virtanen, D. Cournapeau, E. Wieser, J. Taylor, S. Berg, N. J. Smith, R. Kern, M. Picus, S. Hoyer, M. H. van Kerkwijk, M. Brett, A. Haldane, J. F. del Río, M. Wiebe, P. Peterson, P. Gérard-Marchant, K. Sheppard, T. Reddy, W. Weckesser, H. Abbasi, C. Gohlke, and T. E. Oliphant, Array programming with NumPy, *Nature* **585**, 357 (2020).
- [46] The same holds true for the columns due to the Hermitian structure of Hamiltonians.
- [47] J. R. McClean, K. J. Sung, I. D. Kivlichan, Y. Cao, C. Dai, F. Schuyler, C. Gidney, B. Gimby, P. Gokhale, T. Häner, T. Hardikar, V. Havlicek, O. Higgott, C. Huang, J. Izaac, Z. Jiang, X. Liu, S. McArdle, M. Neeley, T. O'Brien, B. O'Gorman, I. Ozfidan, M. D.

- Radin, J. Romero, N. Rubin, N. P. D. Sawaya, K. Setia, S. Sim, D. S. Steiger, M. Stuedtner, Q. Sun, W. Sun, D. Wang, F. Zhang, and R. Babbush, OpenFermion: The Electronic Structure Package for Quantum Computers, arXiv:1710:07629 [10.48550/arXiv.1710.07629](https://arxiv.org/abs/10.48550/arXiv.1710.07629) (2017).
- [48] **Qiskit Nature**, github.com/qiskit-community/qiskit-nature (2025).
- [49] **CUDA-QX**, github.com/NVIDIA/cudaqx (2025).
- [50] V. Berg, J. Izaac, M. Schuld, C. Gogolin, S. Ahmed, V. Ajith, M. S. Alam, G. Alonso-Linaje, B. Akash-Narayanan, A. Asadi, J. M. Arrazola, U. Azad, S. Banning, C. Blank, T. R. Bromley, B. A. Cordier, J. Ceroni, A. Delgado, O. D. Matteo, A. Dusko, T. Garg, D. Guala, A. Hayes, R. Hill, A. Ijaz, T. Isacsson, D. Ittah, S. Jangiri, P. Jain, E. Jiang, A. Khandelwal, K. Kottmann, R. A. Lang, C. Lee, T. Loke, A. Lowe, K. McKiernan, J. J. Meyer, J. A. Montañez, R. Moyard, Z. Niu, L. J. O’Riordan, S. Oud, A. Panigrahi, C.-Y. Park, D. Polatajko, N. Quesada, C. Roberts, N. Sá, I. Schoch, B. Shi, S. Shu, S. Sim, A. Singh, I. Strandberg, J. Soni, A. Száva, S. Thabet, R. A. Vargas-Hernández, T. Vincent, N. Vitucci, M. Weber, D. Wierichs, R. Wiersema, M. Willman, V. Wong, S. Zhang, and N. Killoran, PennyLane: Automatic differentiation of hybrid quantum-classical computations, arXiv:1811.04968 [10.48550/arXiv.1811.04968](https://arxiv.org/abs/10.48550/arXiv.1811.04968) (2018).
- [51] **pyChemiQ**, github.com/OriginQ/pyChemiQ (2025).
- [52] R. Seidel, S. Bock, R. Zander, M. Petrič, N. Steinmann, N. Tcholtchev, and M. Hauswirth, **Qrisp: A framework for compilable high-level programming of gate-based quantum computers** (2024), arXiv:2406.14792.
- [53] T. Helgaker, P. Jørgensen, and J. Olsen, *Molecular Electronic-Structure Theory* (Wiley, 2000).
- [54] **The boost c++ libraries**, www.boost.org (2025).
- [55] **emhash**, <https://github.com/ktprime/emhash> (2026).
- [56] **rapidhash**, <https://github.com/Nicoshev/rapidhash> (2025).
- [57] J. Gray, quimb: A python library for quantum information and many-body calculations, *Journal of Open Source Software* **3**, 819 (2018).

Supplemental Material: A generalized framework for quantum subspace eigenproblems

Paul D. Nation,^{1,*} Abdullah Ash Saki,² and Hwajung Kang¹

¹IBM Quantum, IBM T. J. Watson Research Center, Yorktown Heights, NY 10598 USA

²IBM Quantum, IBM Research Cambridge, Cambridge, MA 02142 USA

(Dated: March 20, 2026)

S1. EXTENDED ALPHABET MERGING RULES

Repeated indices in fermionic Hamiltonian terms can be merged together into a single operator when working over an extended alphabet of projection and ladder operators. The 16 rules used in this merging are presented in Tbl. (S1).

TABLE S1. Complete table of merging rules for combining repeated indices in fermionic terms over the alphabet of projection and ladder operators where $0 \equiv ff^+$, $1 \equiv f^+f$. ‘null’ indicates those outcomes that do not contribute to the output operator.

$-- = ff = \text{null}$	$+- = f^+f \equiv 1$
$0- = ff^+f = f(1 - ff^+) = -$	$1- = f^+ff = \text{null}$
$-+ = ff^+ \equiv 0$	$++ = f^+f^+ = \text{null}$
$0+ = ff^+f^+ = \text{null}$	$1+ = f^+ff^+ = f^+(1 - f^+f) = +$
$-0 = fff^+ = \text{null}$	$+0 = f^+fff^+ = f^+(1 - f^+f) = +$
$00 = ff^+ff^+ = ff^+(1 - f^+f) = 0$	$10 = f^+fff^+ = \text{null}$
$-1 = fff^+f = f(1 - ff^+) = -$	$+1 = f^+f^+f = \text{null}$
$01 = fff^+f^+f = \text{null}$	$11 = f^+ff^+ = f^+f(1 - ff^+) = 1$

S2. RECURSIVE ALGORITHM FOR A MINIMAL PERTURBATIVE SUBSPACE

Here we describe the method used to reduce the subspace dimensionality whilst maintaining a high-accuracy solution. Our technique takes advantage of the fact that many off-diagonal matrix elements, in problems such as those from quantum chemistry, may be markedly smaller in amplitude than the diagonal energy splittings between states, allowing for their contributions to the final eigenenergy to be treated perturbatively. In addition, we utilize the structure of the Hamiltonian, noting that off-diagonal matrix-elements not directly coupled to an initial target subspace are mediated by additional small couplings, the product of which quickly goes to zero. The end result is a Recursive Algorithm that generates a Minimal Perturbative Subspace (RAMPS) around the initial subspace.

To elucidate this method we consider the tri-diagonal Hamiltonian eigenvalue equation:

$$\begin{pmatrix} H_{00} & H_{01} & 0 & 0 \\ H_{10} & H_{11} & H_{12} & 0 \\ 0 & H_{21} & H_{22} & H_{23} \\ 0 & 0 & H_{32} & H_{33} \end{pmatrix} \begin{pmatrix} c_0 \\ c_1 \\ c_2 \\ c_3 \end{pmatrix} = E \begin{pmatrix} c_0 \\ c_1 \\ c_2 \\ c_3 \end{pmatrix}, \quad (\text{S1})$$

where we assume that the 0th-row contains the dominant contribution to the eigenenergy, $E/H_{00} = 1 + \delta/H_{00}$, where δ/H_{00} is a small parameter, and that the off-diagonal terms are smaller than the diagonal energy splittings; we start with an initial subspace consisting of a single bit-string and target energy H_{00} . Our task is to determine the energy shift δ/H_{00} and the form that the interaction takes.

Assuming that the off-diagonal terms are small compared to the energy splittings with the target energy, H_{00} , we arrive at a recursive expression for δ/H_{00} :

$$\begin{aligned} \frac{\delta}{H_{00}} &\simeq \frac{|H_{01}|^2}{H_{00}(H_{00} - H_{11})} \\ &+ \frac{1}{H_{00}(H_{00} - H_{11})} \left[\frac{|H_{01}|^2}{(H_{00} - H_{11})} \frac{|H_{12}|^2}{(H_{00} - H_{22})} \right] \\ &+ \frac{1}{H_{00}(H_{00} - H_{11})(H_{00} - H_{22})} \\ &\times \left[\frac{|H_{01}|^2}{(H_{00} - H_{11})} \frac{|H_{12}|^2}{(H_{00} - H_{22})} \frac{|H_{23}|^2}{(H_{00} - H_{33})} \right] \end{aligned} \quad (\text{S2})$$

The first line in Eq. (S2) yields the shift in energy from terms directly coupled to the target subspace. The remaining lines show the recursive nature of the coupling between bit-strings not directly coupled to the initial subspace, with this interaction mitigated by an increasing number of small off-diagonal matrix-elements leading to imperceptible impact on the final energy.

The expansion in Eq. (S2) can be generalized to work with general Hamiltonians H and input parameters. The simplest scenario, and the one used in this work, is to start with an initial subspace \mathcal{S}_0 , comprised of a single bit-string, and target energy E that is the diagonal energy corresponding to this starting bit-string. However, for Hamiltonians where the target eigenvalue is nearly degenerate and/or the off-diagonal terms cannot be treated perturbatively, i.e. the system is strongly-coupled, \mathcal{S}_0 can be a multi-dimensional subspace and the target energy E would be an eigenvalue found by solving H within \mathcal{S}_0 .

* E-mail: paul.nation@ibm.com

Algorithm 1: RAMPS

Input: An Hamiltonian H partitioned into a set of off-diagonal groups \mathcal{G} , initial subspace \mathcal{S}_0 , target energy E , and tolerance τ .

Output: Modified subspace \mathcal{S}_{out}

```

1 Function RAMPS( $H, \mathcal{S}_0, E, \tau$ )
2    $\mathcal{S}_{\text{out}} \leftarrow \mathcal{S}_0$ 
3   foreach  $b_i \in \mathcal{S}_0$  do
4      $\text{next\_rows} \leftarrow \{b_i\}$            // Next rows
5      $\text{next\_pre} \leftarrow [1/E]$          // Next prefactors
6     while  $\dim(\text{next\_rows}) \neq 0$  do
7        $\text{cur\_rows} \leftarrow \text{next\_rows}$  // Current rows
8        $\text{cur\_pre} \leftarrow \text{next\_pre}$  // Current prefactors
9        $\text{next\_rows} \leftarrow \{\}$ 
10       $\text{next\_pre} \leftarrow []$ 
11       $z \leftarrow 0$  // Counter for prefactor array
12      foreach  $b_j \in \text{cur\_rows}$  do
13        foreach  $g \in \mathcal{G}$  do
14           $b_k \leftarrow \text{COLUMNBITSTRING}(j, g)$ 
15           $\text{amp} \leftarrow \text{cur\_pre}[z] \cdot \frac{|H_{jk}|^2}{(E - H_{kk})}$ 
16          if  $|\text{amp}| > \tau$  then
17            // Add column and prefactor
18             $\text{next\_rows} \leftarrow \text{next\_rows} \cup \{b_k\}$ 
19             $\text{next\_pre.add}(\text{amp}/(E - H_{kk}))$ 
20           $z \leftarrow z + 1$ 
21       $\mathcal{S}_{\text{out}} \leftarrow \mathcal{S}_{\text{out}} \cup \text{next\_rows}$  // Add next rows
22  return  $\mathcal{S}_{\text{out}}$ 

```

For example, if we aim to find the ground state eigenenergy, then the target energy E would be the ground state eigenenergy for H restricted to \mathcal{S}_0 . Together with an user supplied tolerance value τ , these values can be used as the starting point for RAMPS recursion. The general algorithm is presented in Alg. (1).

Algorithm (1) yields a refined output subspace \mathcal{S}_{out} that is comprised of the initial subspace \mathcal{S}_0 together with bit-strings that correspond to matrix elements that shift the target energy value by a relative amount greater than τ . The output subspace is therefore nominally larger than the initial. In practice, this algorithm is modified to terminate the RAMPS process after a maximum number of recursions to prevent the possibility of traversing the full Hilbert space. Because the initial subspace and target energy are necessarily approximations (otherwise the solution would be known), it is possible to use the RAMPS output to generate better a trial subspace \mathcal{S}_0 and associated target energy E for a subsequent RAMPS refinement. In this manner, it is possible to iteratively yield subspaces with increasing overlap with the true eigenstate, and thus more accurate eigenenergies.

In order to directly compare the eigenenergies from RAMPS refinement to those found from working in the

full sampled subspaces we further modify Alg. (1) to limit the recursive search for bit-strings to only those bit-strings found in the full sampled subspace $\mathcal{S}_{\text{full}}$. In particular, line 16 of Alg. (1) is modified to include checking that column bit-string b_k is an element of $\mathcal{S}_{\text{full}}$. With this restriction, typically $\dim(\mathcal{S}_{\text{out}}) \ll \dim(\mathcal{S}_{\text{full}})$, as demonstrated in Sec. (I) of the main text.

S3. MOST-SIGNIFICANT OFF-DIAGONAL BIT

Here we show an illustrative example of how checking just the most significant off-diagonal bit (MSOB) in the row bit-set allows us to detect a lower (or upper) triangle matrix element as described in the main text.

Suppose the row bit-set is 110110, and the `group_offdiag_inds` of a group is [1, 3]. The MSOB is therefore 3, and row bit at the MSOB position is 0 (110110), recalling that bit indexing starts from the right. In the column bit-set, the bit at the MSOB position will be flipped to 1. Now, a column bit-set with 111... will always be greater than the row bit-set 110110 regardless of the trailing bits. As bit-sets are integer sorted in the subspace, a column bit-set greater than the row indicates the corresponding col index is also greater than the row index. When the col index is greater than row index, the matrix element belongs in the upper-triangle, and we can skip matrix element evaluation for the group.

Now, consider the opposite scenario using the same row bit-set but a different group with `group_offdiag_inds` = [1, 2]. Here, the MSOB for this group is 2, and the row bit at MSOB is 1, i.e. (110110). A column bit-set with flipped MSOB, 1100..., will always be smaller than the row bit-set 110110 regardless of the trailing bits. Therefore, the corresponding col index will be smaller than the row index, denoting a lower-triangle matrix element. In FULQRUM we only evaluate matrix-elements in the lower-triangle and in this case would proceed, as discussed in the main text, to determine if the column bit-string is in the subspace, and if so, evaluate the matrix element and populate the corresponding upper-triangle entry in a single pass.

The benefit of the approach is we only need the row bit-set and MSOB of a group to determine which triangle contains the element. This allows us to reject a group without explicit col bit-set computation and subsequent comparison between col and row bit-sets. Moreover, we can avoid touching the full `group_offdiag_inds` during this evaluation by caching collecting MSOB of each group in a vector.